REPORT NO.
UCB/SEMM-90/18

STRUCTURAL ENGINEERING,
MECHANICS AND MATERIALS

A MIXED FORMULATION FOR THE FINITE ELEMENT SOLUTION OF CONTACT PROBLEMS

by

PANAYIOTIS PAPADOPOULOS

and

ROBERT L. TAYLOR

SEPTEMBER 1990

DEPARTMENT OF CIVIL ENGINEERING
UNIVERSITY OF CALIFORNIA
BERKELEY, CALIFORNIA

A MIXED FORMULATION FOR THE FINITE ELEMENT SOLUTION OF CONTACT PROBLEMS

Panayiotis PAPADOPOULOS and Robert L. TAYLOR

Department of Civil Engineering, University of California at Berkeley, Berkeley, CA 94720, U.S.A.

Contents

Abstract

In this paper we present a finite element algorithm for the static solution of two-dimensional frictionless contact problems involving bodies undergoing arbitrarily large motions and deformations. A mixed penalty formulation is employed in approximating the resulting variational inequalities. The algorithm is applied to quadratic elements along with a rational scheme for determining the contacting regions. Several numerical simulations illustrate the applicability and accuracy of the proposed solution procedure.

1. Introduction

Mechanical contact is of considerable importance in a wide range of engineering applications. The interaction of contacting bodies introduces 'unilateral' constraints on their relative displacements. Indeed, the above constraints are enforced only on parts of their boundaries where contact actually occurs and become inactive where the bodies are apart from one another. Analytical methods have provided solutions only for restricted classes of problems, [1,2], owing largely to lack of a priori knowledge of the exact contact surfaces.

The unilateral nature of the boundary conditions gives rise to variational principles realized in the form of inequalities, [3]. In treating inequality constraints emanating from mechanical contact, several numerical algorithms have been proposed, primarily in conjunction with the finite element method. There appear to exist two main directions in attacking the discrete contact problem; the one uses special optimization techniques for the resulting non-linear mathematical programming problem, [4-6], while the other directly transforms the inequalities to equalities by enforcing the constraint conditions through penalty, [7], or augmented Lagrangian formulations, [8]. Even though one can reasonably argue that penalty and augmented Lagrangian schemes are optimization techniques in their own right, they are viewed here separately from other special techniques, because of their simplicity, generality and capability for direct and efficient computer implementation.

In this paper, we use a penalty formulation. A pivotal issue in this approach is the choice of pressure approximation. Typically, the contact pressure is approximated with reference to its value at the nodal points of the discretized bodies. Contact problems involving small deformations are adequately treated by an assumption of node-to-node contact, [9]. For bodies undergoing large motions the above assumption is too restrictive and one has to allow for node-on-surface contact, [10]. The main drawback of nodal contact is that it only enforces the non-penetration condition in a discrete number of points on the boundary, while, at the same time, variationally consistent pressures are not assumed at the outset along the contact surface; instead, nodal forces are computed and, subsequently, tributary area methods are used to transform them into equivalent pressures. An alternative approach based on a perturbed Lagrangian functional, makes an explicit assumption for the approximation of the pressure field and enforces the non-penetration condition in an average sense over a well-defined segment of the boundary, [11].

The formulation proposed here is developed for the fully non-linear two-dimensional kinematics and, therefore, is automatically applicable to contact problems involving large deformations, as well as non-linear interface material constitutions. The cornerstone of the approximation is a three field mixed principle according to which displacements, pressures and gaps (penetrations) are independently approximated along the contact slideline. Quadratic elements are used throughout the analysis and an elaborate scheme of uniquely defining the contact elements is presented.

2. The continuum problem

Consider two deformable bodies with reference configurations B^1, B^2 and smooth boundaries ∂B^1, ∂B^2, respectively, with reference to a fixed Cartesian coordinate system $\mathbf{x}(x, y)$, see Fig. 2.1 . The boundary of each body is uniquely decomposed into three mutually disjoint subregions according to

$$\partial B^k = \partial B_u^k \bigcup \partial B_t^k \bigcup C \ , \ k=1,2 \ ,$$

where boundary displacements $\bar{\mathbf{u}}^k$ are specified on ∂B_u^k, surface tractions $\bar{\mathbf{t}}^k$ are specified on ∂B_t^k, while on C the two bodies come into contact. On C the two bodies possess a common normal denoted by $\mathbf{n}^1 = -\mathbf{n}^2$, where $\mathbf{n}^k$ is the outer unit normal to B^k. Moreover, consider the displacement fields and body forces

$$\mathbf{u}^k = \mathbf{u}^k(\mathbf{x}) \ ,$$

$$\mathbf{f}^k = \mathbf{f}^k(\mathbf{x}) \ ; \ \mathbf{x} \in B^k \ , \ k=1,2 \ .$$

The non-penetration condition along C requires that

$$h = [(\mathbf{x}^2 + \mathbf{u}^2) - (\mathbf{x}^1 + \mathbf{u}^1)] \cdot \mathbf{n}^1 = 0 \ , \tag{2.1}$$

where h represents the gap (penetration) in the current configuration. Equation (2.1) poses a constraint on the relative motion of the two bodies. A contact pressure p acts on C so that the contact boundary conditions may be written in a Kuhn-Tucker form as

$$p\, h = 0 \ , \ p \le 0 \ , \ h \ge 0 \ . \tag{2.2}$$

We independently define the space of trial functions for the displacements as V and the pressure as P according to

$$V = V^1 \times V^2 \ ; \ V^k = \left\{ \mathbf{v} \in (H^1(B^k))^2 \mid \mathbf{v}(\mathbf{x}) = \mathbf{0} \ , \ \mathbf{x} \in \partial B_u^k \right\} \ , \ k=1,2 \ ,$$

$$P = \left\{ q \in H^0(C) \mid q \leq 0 \right\}.$$

It can be easily inferred that any solution $(\mathbf{u}^1, \mathbf{u}^2, p)$ of the contact boundary value problem extremizes the total potential energy functional Π given by

$$\Pi(\mathbf{u}^1, \mathbf{u}^2, p) = \tag{2.3}$$
$$\sum_{k=1}^{2} \left[\int_{B^k} W^k dV - \int_{B^k} \mathbf{f}^k \cdot \mathbf{u}^k dV - \int_{\partial B_t^k} \bar{\mathbf{t}}^k \cdot \mathbf{u}^k d\Gamma \right] - \int_C p \, h(\mathbf{u}^1, \mathbf{u}^2) \, d\Gamma \ ,$$

where W^k stands for the stored (elastic) energy of body k. Note that equation (2.1) is incorporated into the functional form of the total potential energy in (2.3), allowing the unconstrained variation of the trial displacements.

For the purpose of the forthcoming finite element approximation, we define a mixed penalty functional Π_ϵ as

$$\Pi_\epsilon(\mathbf{u}^1, \mathbf{u}^2, p, g) = \Pi(\mathbf{u}^1, \mathbf{u}^2) + \int_C \tfrac{1}{2}\epsilon g^2 d\Gamma + \int_C p \, (h(\mathbf{u}^1, \mathbf{u}^2) - g) \, d\Gamma \ , \tag{2.4}$$

where $\epsilon > 0$ is a preset penalty parameter and g is an independently assumed variable defining the penetration along C, whose space of admissible variations G is given by

$$G = \left\{ g \in H^0(C) \mid g \leq 0 \right\}$$

The value of the penalty parameter is generally proportional to the stiffness of the contacting bodies. Variation of the functional in (2.4) with respect to p and g gives rise to the Euler equations

$$\int_C \delta p \, (h(\mathbf{u}^1, \mathbf{u}^2) - g) \, d\Gamma = 0 \tag{2.5}$$

and

$$\int_C \delta g \, (\epsilon g - p) \, d\Gamma = 0 \ , \tag{2.6}$$

respectively. Equation (2.5) maintains that the displacement-based penetration h must be equal to the independently assumed penetration g in a weak sense over the contact boundary C. Equation (2.6) will be used in recovering variationally consistent pressures from g.

Assuming the choice of finite element subspaces leads to an approximation of g that weakly converges to the 'real' penetration h under successive mesh refinement, the penalty functional in (2.4) will enforce weak satisfaction of (2.1). Clearly, the larger the penalty parameter ϵ, the more accurate the satisfaction of (2.1).

Remarks

- The continuum problem, as well as its numerical solution, can be trivially generalized for the case of multiple bodies in contact.
- An augmented Lagrangian formulation can be easily established by considering the functional Π_{AL} defined according to

$$\Pi_{AL}(\mathbf{u}^1, \mathbf{u}^2, p, g, \lambda) = \Pi_{\epsilon}(\mathbf{u}^1, \mathbf{u}^2, p, g) + \int_C \lambda\, h(\mathbf{u}^1, \mathbf{u}^2)\, d\Gamma$$

where λ is a Lagrange multiplier, [8,12].

3. Slideline considerations

3.1 *A discretization of the contact slideline*

A well-defined approximation of the kinematics of the contact slideline is critical in rendering the algorithm robust and reliable. Ideally, a discretization of C should preserve the basic geometric characteristics of the contacting regions and allow for computationally efficient, unbiased treatment of all cases of potential element contact. Departing from the concept of nodal contact, it is apparent that 'contact elements' must be directly related to continuous parts of the element boundaries. Following [11], these elements will be referred to as *segments*. Appropriate identification of the contact segments can significantly facilitate satisfaction of the discrete counterparts of the constraint equations (2.5) and (2.6). The proposed slideline logic is applicable to both one- and two-dimensional finite elements. In what follows, attention is focused to the case of quadratic elements. Naturally, a similar approach can be easily obtained for linear elements.

Initially, we specify for each body the part of its boundary which is candidate for contact. These surfaces consist of element edges from each body. The next step involves projecting the outer two nodes of element edges from one body onto the boundary of the other, see Fig. 3.1 . This procedure can be carried out by means of an elementary Newton scheme or by solution of a closed-form cubic equation. Subsequently, a search strategy is initiated in order to decide what are the actual contact segments to be further considered in the analysis. Figure 3.2 illustrates all the basic

cases that are potentially encountered in determining segmental acceptance or rejection (all other cases are reducible to these by either symmetry or by exchanging the roles of the two bodies). A summary of the implementation of the above search algorithm is given in Box 1.

Box 1 : Summary of search algorithm for contact segments

1. Input nodes of potential contact surfaces.
2. Loop over element edges of body 1.
3. Loop over element edges of body 2.
4. Compute projections of element edges of body 2 onto body 1.
5. Compute projections of element edges of body 1 onto body 2.
6. Check resulting segment for acceptance/rejection.
7. If edge from body 2 fully projected, go to 3
   Else go to 2
8. When element edges are exhausted, stop.

Interestingly, this process leads to an unbiased definition of segments, in the sense that the actual direction of the search scheme (left-to-right or vice-versa) is immaterial, since, in either case, the same segments will be eventually determined. In addition, each segment contains, by construction, information pertaining to only one element from each of the contacting bodies. This simplifies programming substantially.

In order to compute the surface integrals obtained by invoking stationarity of the discrete counterpart of (2.4), a precise definition of the finite element approximation of C is required. The boundary of either one of the contacting bodies (or even a linear interpolation between their surfaces) can be used for this purpose. Therefore, we define C_h such that

$$C \approx C_h = \bigcup_{i=1}^{N} C_h^i$$

where N is the total number of segments accepted according to the previously described strategy. Our computational experience suggests that, given the segments, the specific choice of contact surface does not substantially affect the numerical results. For convenience, we identify C_h with one of the surfaces, so that the local

coordinate system used for each segment coincides with an appropriate element natural coordinate system. Therefore, we obtain a unique set of segmental end points P and segments ∂C_h^i determined by P.

For each segment, necessary information is retained for later use in computing the finite element matrices. This includes values of the local coordinate for the segmental end points and integration points, as well as cartesian coordinates of the normals to the segmental surface at the above points.

Finally, for consistency with the finite element fields to be specified, a unique normal to the contact boundary must be determined at each of the outer two nodes of the elements participating in the contact calculations. This is because finite elements guarantee only C^0 continuity of the displacements at these nodes, as illustrated in Fig. 3.3 . A unique normal can be computed by averaging the normals obtained at a shared node between two adjacent element edges.

4.2 *Contact/release condition*

Contact/release conditions are monitored for each contact segment at every iteration (i+1) within a global step of the solution as follows;

Box 2 : Contact/release conditions

At local iteration (i+1)

Loop over integration points

compute trial penetration $\hat{g}^{(i)}$

if $\hat{g}^{(i)} \leq 0 \rightarrow g^{(i)} = \hat{g}^{(i)}$

if $\hat{g}^{(i)} > 0 \rightarrow g^{(i)} = 0$

End loop

Note that contact/release checks are conducted at every integration point *separately*, i.e. partial contact within a single segment is permissible. This is a desirable feature, since it allows the decision of contact/release to be made at discrete points rather than at the segmental level.

Remark

- Element local coordinate systems are used in computing projections of nodes to element edges, as well as in deciding for the acceptance/rejection of potential segments according to Fig. 3.2 .

4. The discrete problem

The proposed finite element approximation of contact boundary value problems is based on the functional in (2.4). The sequence of steps to be followed in the proposed formulation begins with the solution of (2.5) for g in terms of the displacements of the two bodies. Subsequently, extremization of (2.4) with respect to the same displacements gives rise to a system of (generally non-linear) equations with $\mathbf{u}^1, \mathbf{u}^2$ as the only unknowns to be determined. Finally, variationally consistent pressures are recovered from (2.6).

We define finite element subspaces V_h, P_h and G_h for the independent fields that appear in the variational statement as follows;

$$V_h = V_h^1 \times V_h^2 \quad ; \quad V_h^k = \left\{ \mathbf{v} \in P_0^2(B^k) \mid \mathbf{v}(\mathbf{x}) = \mathbf{0} \ , \ \mathbf{x} \in \partial B_u \right\} \ , \ k=1,2 \ ,$$

$$P_h = \left\{ p \in P_{-1}^2(C_h) \mid p \leq 0 \right\}$$

and

$$G_h = \left\{ g \in P_0^2(C_h) \mid g \leq 0 \right\} \ ,$$

where P_k^n denotes a polynomial of degree n with derivatives up to order k. Note that all three fields are piecewise quadratic. Moreover, displacements and penetration are continuous in a natural coordinate system along the contact boundary C_h, while pressure is allowed to be discontinuous. The constraint equations (2.5) and (2.6) will be satisfied for each contact segment separately.

We now introduce a restriction $\tilde{G}_h$ to G_h by collocating g and h at the segmental end points,

$$\tilde{G}_h = \left\{ g \in P_0^2(C_h) \mid g \leq 0 \ , \ g = h(\mathbf{x}, \mathbf{v}) \ , \ \mathbf{x} \in P \right\} \ ,$$

where

$$\mathbf{v} = \left[\mathbf{v}^1 \quad \mathbf{v}^2 \right]^T \ .$$

In addition to the above finite element approximation, equations (2.5) and (2.6) will be satisfied by way of a reduced integration scheme, and, particularly, Simpson's rule. Therefore, from (2.5) it is deduced that for each segment

$$g = \tfrac{1}{2}\xi(\xi-1)h_l + \tfrac{1}{2}\xi(\xi+1)h_r + (1-\xi^2)h_c \quad , \tag{4.1}$$

where ξ is a local natural coordinate system defined in the previous section and h_l, h_r and h_c are the ordinates of the displacement-based penetration h at the left, right and center of the segment, respectively.

Furthermore, equation (2.6) will be satisfied exactly under the assumption that

$$p = \tfrac{1}{2}\xi(\xi-1)p_l + \tfrac{1}{2}\xi(\xi+1)p_r + (1-\xi^2)p_c \quad , \tag{4.2}$$

where, again, p_l, p_r and p_c denote the pressures at the left, right and center of the segment, respectively. Finally, variation of the functional in (2.4) with respect to $\mathbf{v}$ yields a residual $\mathbf{R}$ due to the total potential energy of the two bodies together with a contact residual $\mathbf{R}_c$ given by

$$\mathbf{R}_c \cdot \delta\mathbf{v} = \int_{C_c} p\,\delta h \; d\Gamma \quad , \tag{4.3}$$

A contact stiffness $\mathbf{K}_c$ is computed from (4.3) by means of linearization of $\mathbf{R}_c$. The non-linear problem takes the form

$$\mathbf{u}^{(i+1)} = \mathbf{u}^{(i)} + \Delta\mathbf{u}^{(i)} \quad ,$$

where $\Delta\mathbf{u}^{(i)}$ is computed from

$$\sum(\mathbf{K}^{(i)} + \mathbf{K}_c^{(i)})\,\Delta\mathbf{u}^{(i)} = \mathbf{R}^{(i)} + \mathbf{R}_c^{(i)} \tag{4.4}$$

and is solved incrementally by a full Newton scheme. In (4.4) $\mathbf{K}^{(i)}$ results from the linearization of $\mathbf{R}^{(i)}$ with respect to $\mathbf{v}$ and the summation symbol is understood in the sense of the direct stiffness method. Simpson's rule is used for the integration of all contact element matrices.

For the special case of the Signiorini problem, a similar approximation has been proposed in [13].

Remarks

- An important feature of the above solution strategy is that all contact calculations can be conducted at the local segmental level, therefore substructuring or other computationally expensive global procedures along the slideline are not necessary.
- From (2.6) it follows that

  $$p = \epsilon g$$

  pointwise. The variable that enters the formulation as a Lagrange multiplier is

the assumed penetration g, rather than the pressure p. Continuity of g is a highly desirable property, because together with the definition of the contact segments guarantees that the total number of constraints involved in the satisfaction of the non-penetration condition never exceeds the number of available displacement equations. The above statement is valid even if one of the two contacting bodies is rigid (i.e., it possesses no active degrees of freedom). In that sense, the algorithm passes the mixed patch test proposed in [14]. At this point, a crucial distinction has to be made between mechanical contact and other frequently encountered constrained problems, such as incompressibility. Contact imposes constraints on a part of the boundary displacement unknown before the solution, while incompressibility and all the other constitutive constraints pose restrictions to the deformation that hold *ab initio* throughout the body. Application of the mixed patch test to contact problems presupposes that the contacting surfaces are known in advance and this, of course, is not, in general, true.

- In the case where actual pressure distribution must be discontinuous (e.g. contact of a body composed of two different materials with a rigid surface), the computed pressure will be also discontinuous, since the penalty parameter ϵ will account for the change in the material properties.
- Classical nodal contact can be easily recovered from the functional in (2.4) and the previously assumed fields by simply redefining the gap g according to

$$g = \sum_I g_I \delta(\mathbf{x}_I) \ ,$$

where $\delta(\cdot)$ denotes the Dirac delta function and $\mathbf{x}_I$ are the nodal coordinates along the contact slideline. The one-pass (resp. two-pass) algorithm is obtained by considering the nodes of one (resp. both) bodies in the definition of $\mathbf{x}_I$.

5. Numerical simulations

A series of numerical simulations have been performed to evaluate the robustness, accuracy and applicability of the proposed formulation. Computations have been performed within the environment of the Finite Element Analysis Program (FEAP), see Chap. 15 of [15].

5.1 *A patch test*

A flexible punch comes in contact with a deformable foundation as in Fig. 5.1.1 . Uniform loading q=1.0 is applied on the free upper surface of both the punch and the foundation. Plane strain conditions and linear elasticity are assumed. The elastic constants in the computations are

$$E_{pun} = E_{foun} = 10^5 \quad , \quad \nu_{pun} = \nu_{foun} = 0.3$$

and the penalty parameter is set to $\epsilon = 10^8$. This problem tests the capability of the formulation to allow transmission of constant pressure through the contact surface. The patch test is passed for the symmetric, unsymmetric and distorted meshes of Fig. 5.1.2 .

5.2 *Rigid punch on an elastic foundation*

A rigid punch is indented into an elastic foundation in plane strain by means of a forced vertical displacement v=0.05, see Fig. 5.2.1 . Meshes used are shown in Fig. 5.2.2 . This problem has a closed form solution for the case of a semi-infinite elastic domain, see, e.g., [2]. Note that the pressure field derived from the elasticity solution is singular at the end points of the punch.

The elastic parameters used in the computations are

$$E_{foun} = 100 \quad , \quad \nu_{foun} = 0.3$$

and the penalty parameter is $\epsilon = 10^8$. Pressures computed by the finite element approximations are plotted in Fig. 5.2.3 . Due to the finite discretization of the semi-infinite domain and the point singularity exhibited by the exact pressure field, the variationally consistent pressure is expected to converge slowly and non-uniformly. However, with mesh refinement we obtain fairly smooth pressures within the contact region, and also, as expected, steeper pressure gradients near the singularity.

Figure 5.2.4 underlines the importance and sensitivity of meshing in tackling singular problems as the one at hand. In MC2 the corner nodes of the punch contact a generic point of the foundation, while in MC3 they meet a nodal point. Clearly, MC3 produces a much smoother pressure field than MC2. Finally, the deformed shape for mesh MC4 is illustrated in Fig. 5.2.5 .

5.3 *Elastic punch on elasto-plastic foundation*

The elastic punch of problem 5.1 bearing a uniform load on its top, comes in contact with an elastoplastic foundation, see Fig. 5.3.1 . Plane strain conditions are

enforced along with J_2 constitutive assumption with linear isotropic hardening for the foundation. Furthermore, both bodies are assumed nearly incompressible, so that a B-bar formulation is employed to bypass volumetric locking. The material constants are for the foundation

$$E_{foun} = 10^3 \quad , \quad \nu_{foun} = 0.499 \quad , \quad \sigma_y = 5 \ ,$$

and the coefficient of hardening is $H = 50$. For the punch we use

$$E_{pun} = 10^4 \quad , \quad \nu_{pun} = 0.499 \ .$$

The penalty parameter is taken to be $\epsilon = 10^7$.

The mesh used in the analysis and the final deformation of the two bodies are displayed in Fig. 5.3.2 and Fig. 5.3.3, respectively, while the areas of yielding for several steps during the analysis are presented in Fig. 5.3.4 .

5.4 *Cylinder on rigid foundation*

A long cylinder is pressed against a rigid foundation, as in Fig. 5.4.1 . This is a classical problem for which there exists an approximate theoretical solution for the pressure distribution due to Hertz, see e.g. [1]. One quarter of the mesh is discretized and subjected to a uniform load, as shown in Fig. 5.4.2 . Plane strain conditions are maintained and the material constants used are

$$E_{cyl} = 500 \quad , \quad \nu_{cyl} = 0.3$$

with a penalty parameter of $\epsilon = 10^6$. Despite the coarseness of the mesh, the pressure distribution and the length of contact are in good agreement with the theoretical results, as demonstrated in Fig. 5.4.3 . Furthermore, the deformed shape of the cylinder corresponding to the final loading step is given in Fig. 5.4.4 .

5.5 *Ring on elastic foundation*

A cylindrical ring shown in Fig. 5.5.1 is squeezed between two elastic sheets in plain strain. Due to symmetry, one quarter of the mesh is discretized and a uniform displacement v is applied on the horizontal symmetry line of the ring, see Fig. 5.5.2. In this problem we test the behavior of the algorithm in the presence of large deformations. The material is assumed elastic compressible Neo-Hookean with properties

$$E_{ring} = 10^3 \quad , \quad E_{sheet} = 10^5 \quad , \quad \nu_{ring} = \nu_{sheet} = 0.3 \ .$$

Pressure distributions, Fig. 5.5.3, and corresponding deformed bodies, Fig. 5.5.4, are reported.

Remarks

- For all plots of pressure fields above, we report the computed pressures at the integration points only. However, it is understood from (4.2) that the pressure varies quadratically within each segment.
- The finite element approximations obtained for the above problems are in general satisfactory. The formulation allows for the use of fairly high penalty parameters ($\epsilon \approx 10^2\bar{E}$ to $10^5\bar{E}$, where $\bar{E}$ is an average value of Young's modulus for the deformable bodies in contact) without a significant reduction in the convergence rate. However, in order to speed up convergence, it is at times necessary to progressively increase the penalty parameter from $\epsilon \approx \bar{E}$ up to its final value.

Conclusion

A finite element formulation for the solution of frictionless contact problems involving arbitrary motions of the contacting bodies is presented. The formulation consists of a geometrically consistent and directionally unbiased scheme for determination of the potential contact segments and a mixed penalty interpolation involving displacements, pressures and gaps along the contact slideline. Reduced integration is employed for the contact matrices in order to achieve stable and converging approximations. Numerical experimentation indicates that the above desirable properties are attained.

Acknowledgements

This work has been supported by the Lawrence Livermore National Laboratory under contract Nr. W-7405-ENG-48. The continuous interest of Dr. G.L. Goudreau of LLNL is especially acknowledged. Also, the help of Prof. J.L. Sackman is greatly appreciated.

References

[1] W. Goldsmith, *Impact*, Arnold, London, (1960).

[2] G.M.L. Gladwell, *Contact Problems in the Classical Theory of Elasticity*, Sijthoff & Noordhoff, Alphen aan den Rijn, (1980).

[3] G. Duvaut and J.L. Lions, *Inequalities in Mechanics and Physics*, Springer, Berlin, (1976).

[4] T.F. Conry and A. Seireg, "A Mathematical Programming Method for Design of Elastic Bodies in Contact", *J. Appl. Mech.*, 38, pp. 387-392, (1971).

[5] P.D. Panagiotopoulos, "A Nonlinear Programming Approach to the Unilateral Contact- and Friction-boundary Value Problem in the Theory of Elasticity", *Ing. Arch.*, 44, pp. 421-432, (1975).

[6] J.J. Kalker, "Contact Mechanical Algorithms", *Comm. Appl. Num. Meth.*, 4, pp. 25-32, (1988).

[7] J.T. Oden, "Exterior Penalty Methods for Contact Problems in Elasticity", in *Europe-US Workshop: Nonlinear Finite Element Analysis in Structural Mechanics*, (ed. Bathe, Stein and Wunderlich), Springer, Berlin, (1980).

[8] J.A. Landers and R.L. Taylor, "An Augmented Lagrangian Formulation for the Finite Element Solution of Contact Problems", *SESM Rep.*, 85/09, Univ. California, Berkeley, (1985).

[9] T.J.R. Hughes, R.L. Taylor, J.L. Sackman, A. Curnier and W. Kanoknukulchai, "A Finite Element Method for a Class of Contact-impact Problems", *Comp. Meth. Appl. Mech. Engr.*, 8, pp. 249-276, (1976).

[10] J.O. Hallquist, "NIKE2D: A Vectorized, Implicit, Finite Deformation, Finite Element Code for Analyzing Static and Dynamic Response of 2-D Solids", *UCID rep.*, 19677 (rev.1), Univ. California, Lawrence Livermore National Laboratories, (1986).

[11] J.C. Simo, P. Wriggers and R.L. Taylor, "A Perturbed Lagrangian Formulation for the Finite Element Solution of Contact Problems", *Comp. Meth. Appl. Mech. Engr.*, 50, pp. 163-180, (1985).

[12] R. Glowinski and P. Le Tellec, *Augmented Lagrangian and Operator-Splitting Methods in Nonlinear Mechanics*, SIAM, Philadelphia, (1989).

[13] N. Kikuchi and Y.J. Song, "Penalty/Finite Element Approximations of a Class of Unilateral Problems in Linear Elasticity", *Quart. Appl. Math.*, 39, pp. 1-22, (1981).

[14] O.C. Zienkiewicz, S. Qu, R.L. Taylor and S. Nakazawa, "The Patch Test for Mixed Formulations", *Int. J. Num. Meth. Engr.*, 23, pp. 1873-1883, (1986).

[15] O.C. Zienkiewicz and R.L. Taylor, *The Finite Element Method*, 4th ed., Vol.1, McGraw-Hill, London, (1989).

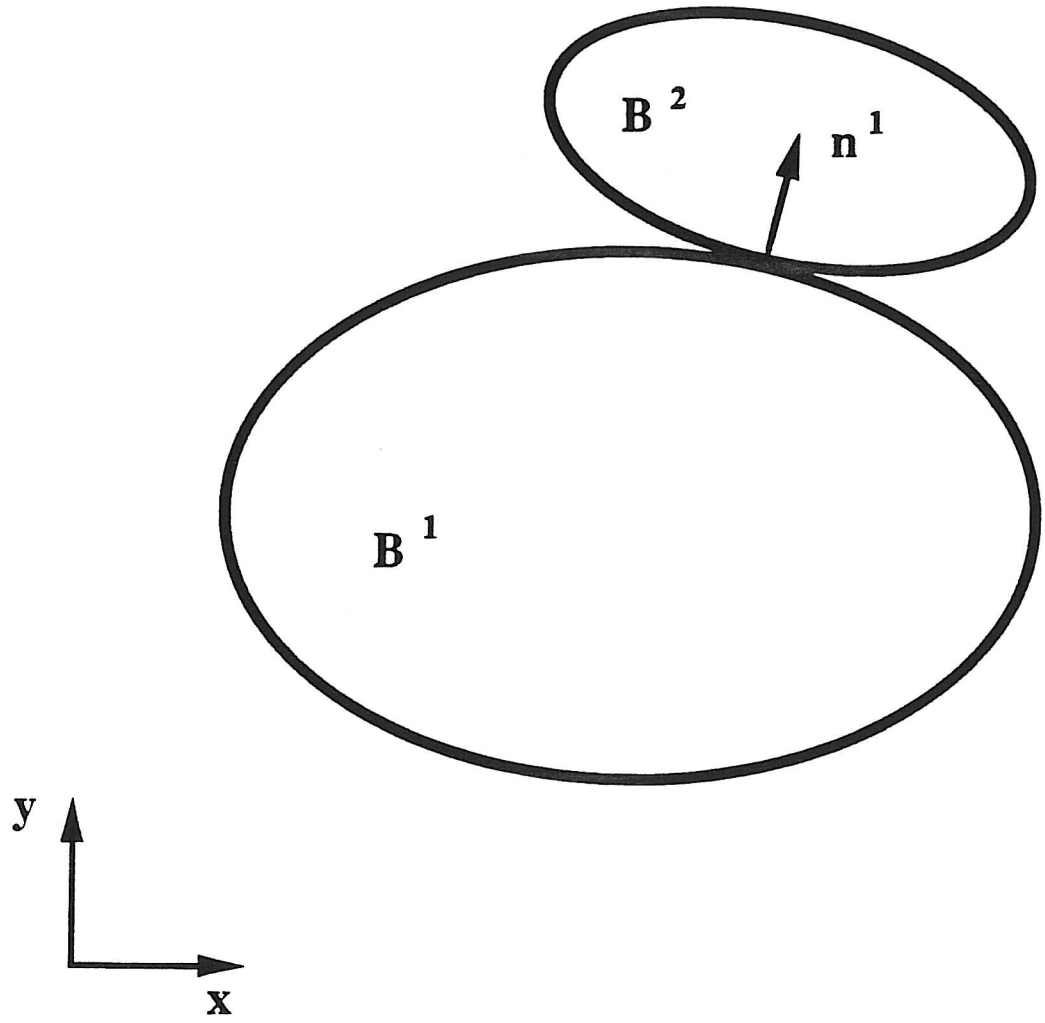

Fig. 2.1 Two-body contact problem

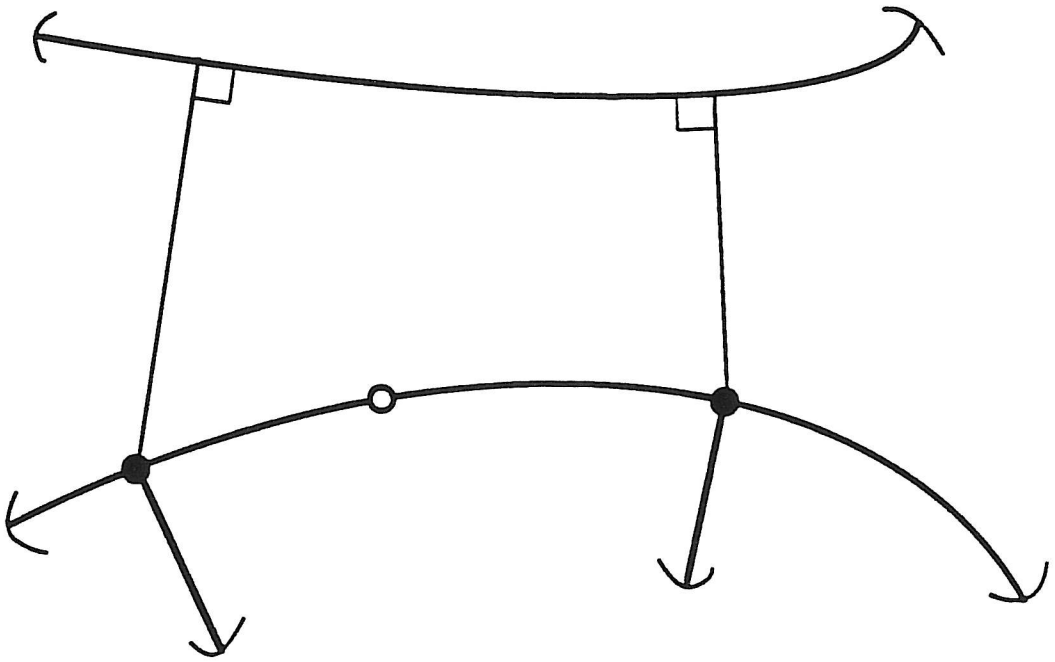

Fig. 3.1 Projection of element edge onto opposite body

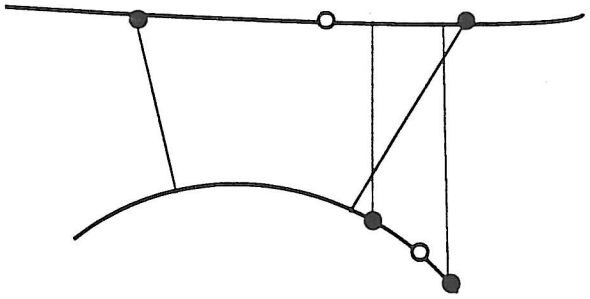

No segment

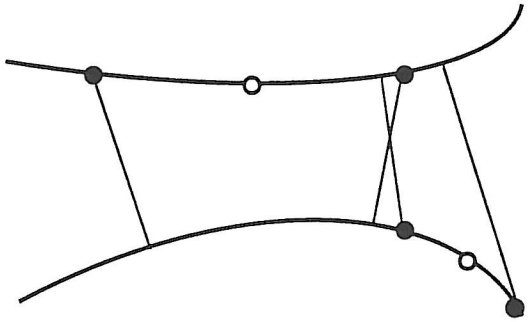

No segment

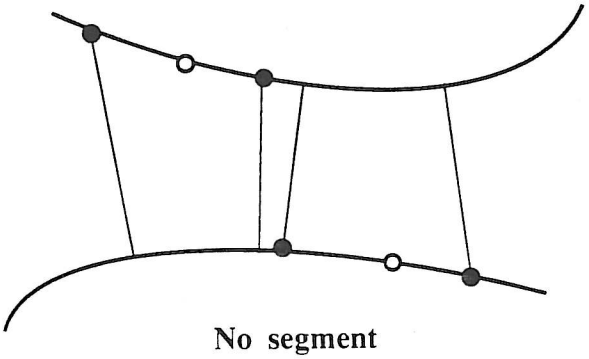

No segment

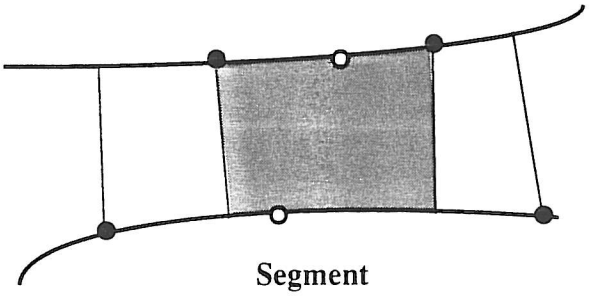

Segment

Fig. 3.2 Segmental acceptance/rejection

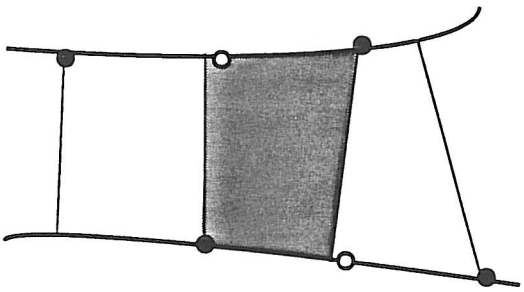

Segment

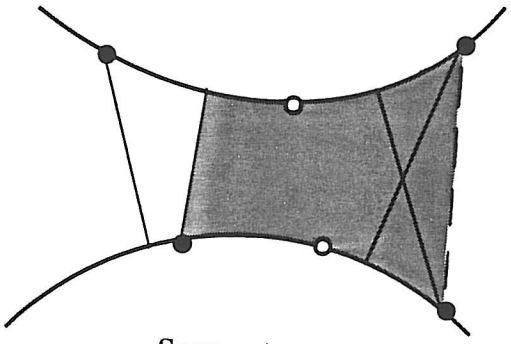

Segment

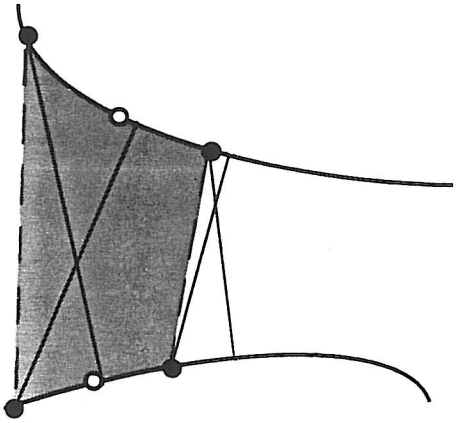

Segment

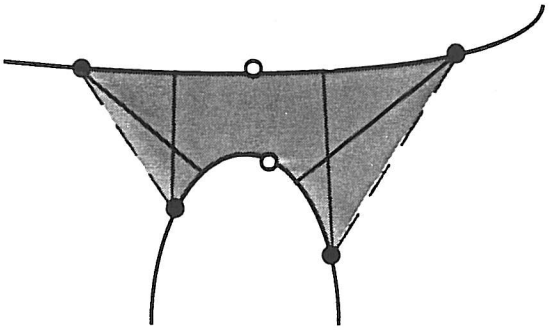

Segment

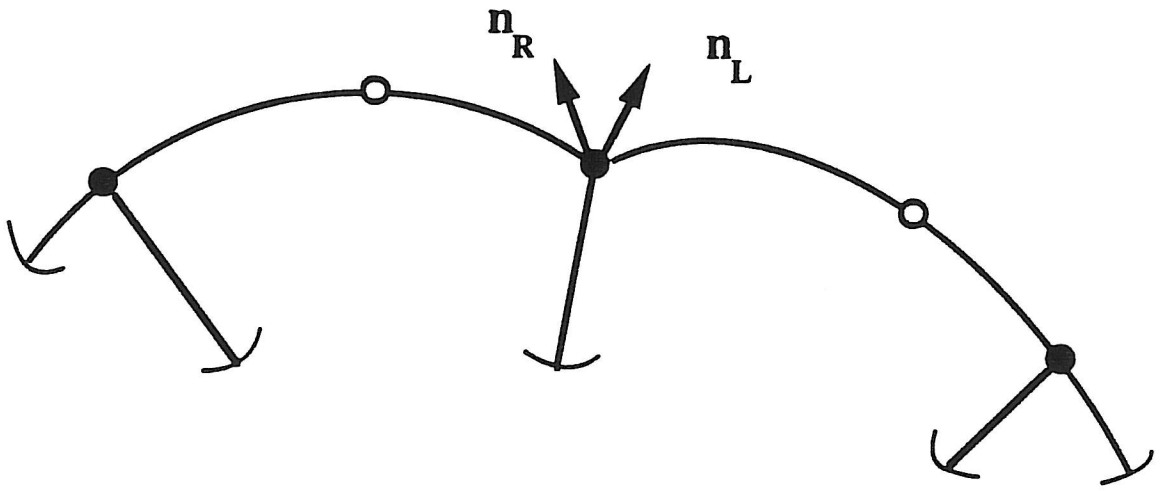

Fig. 3.3 Uniqueness problem for normal to the contact boundary

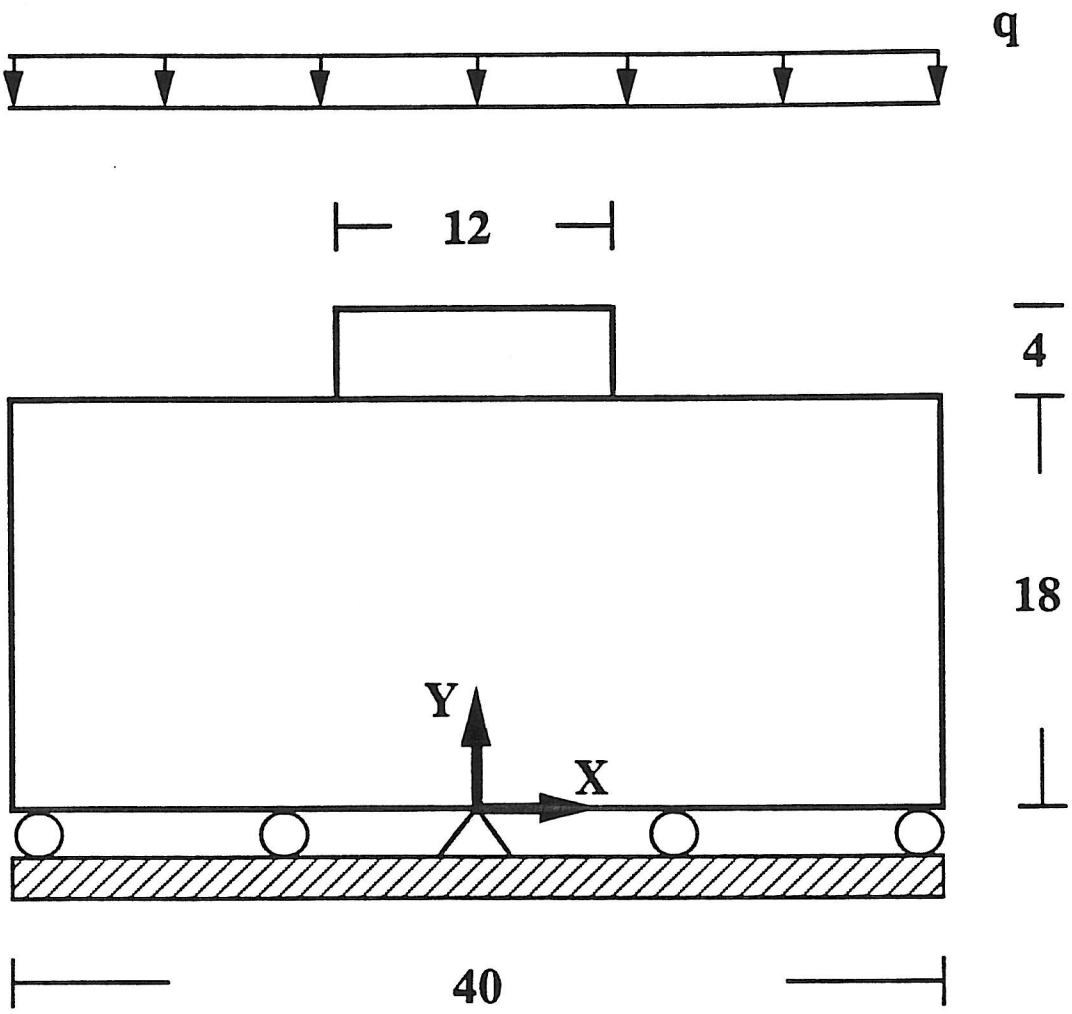

Fig. 5.1.1 Patch test problem

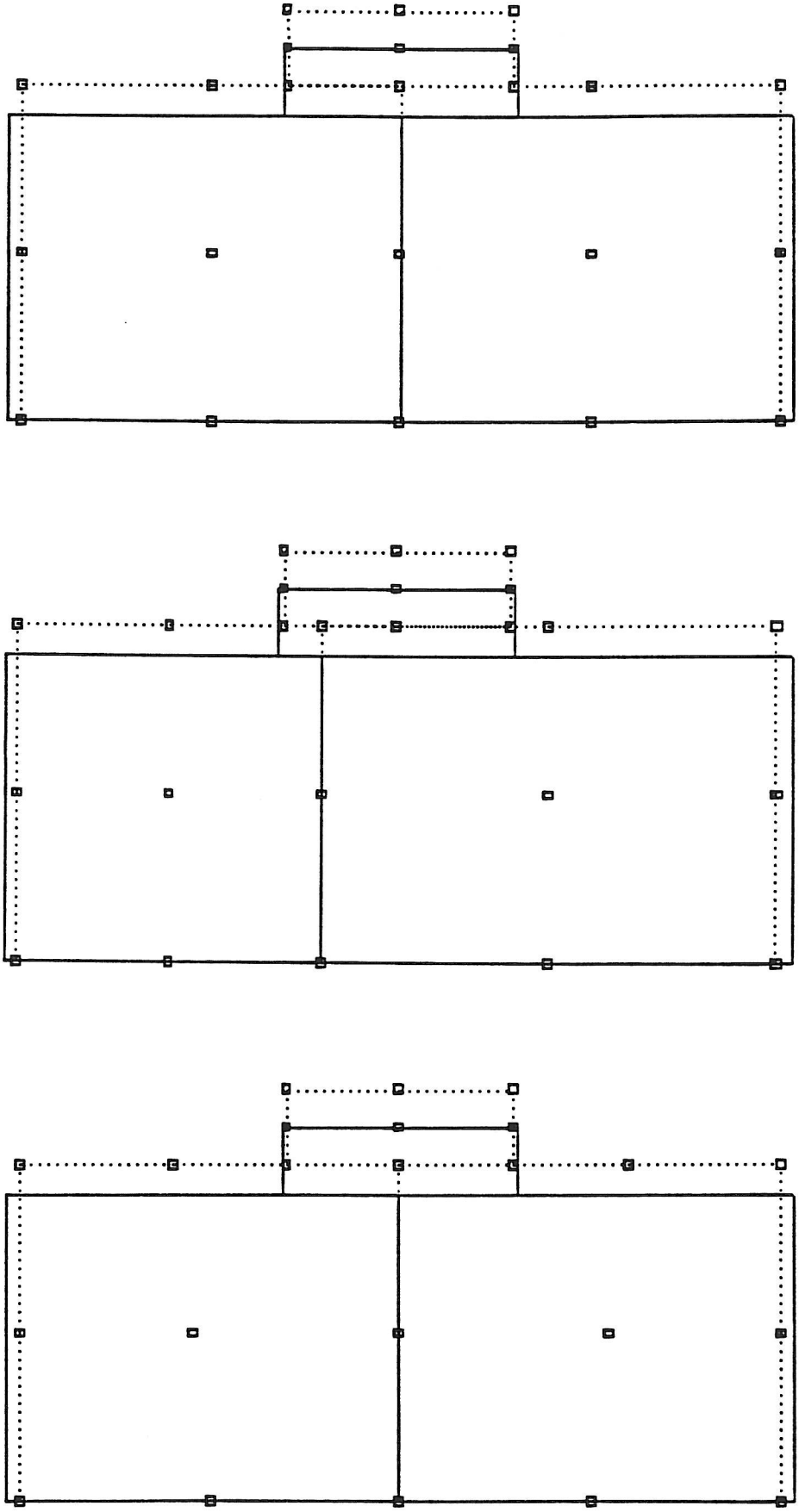

Fig. 5.1.2 Meshes and deformed shapes for patch test

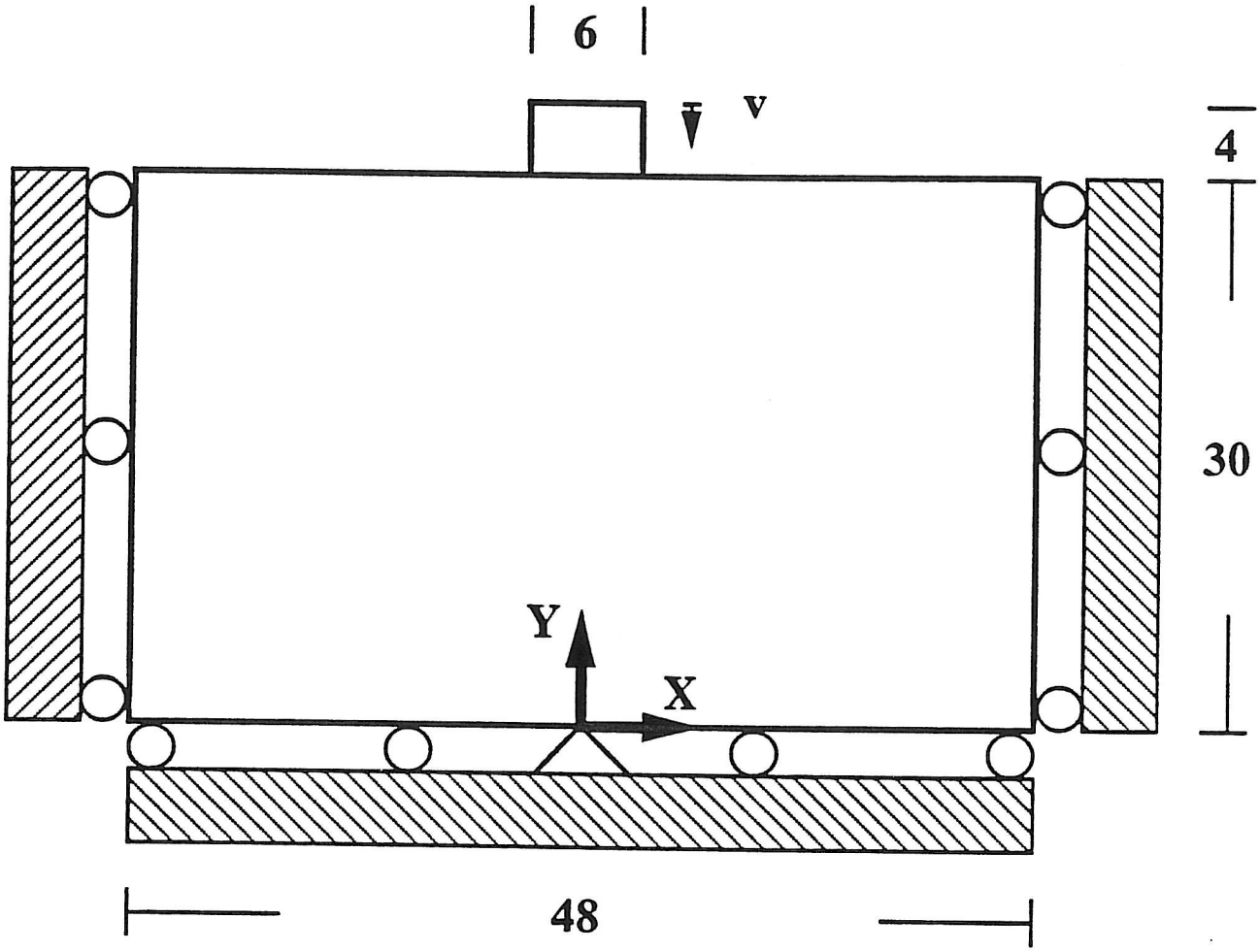

Fig. 5.2.1 Rigid punch on elastic foundation

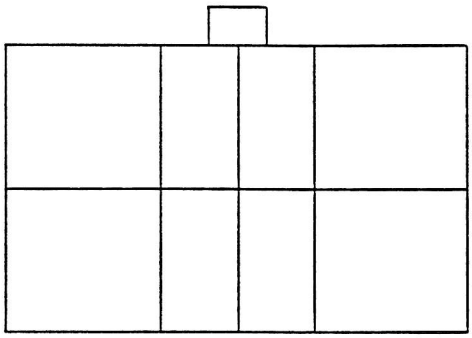

MC1

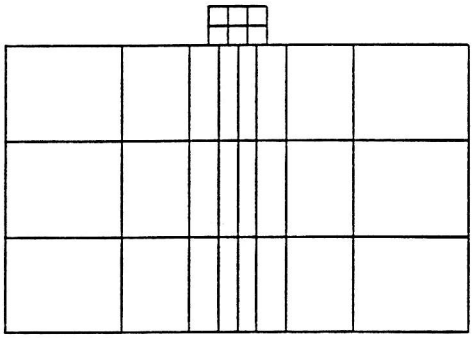

MC2

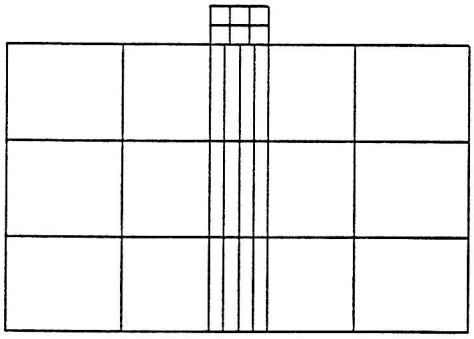

MC3

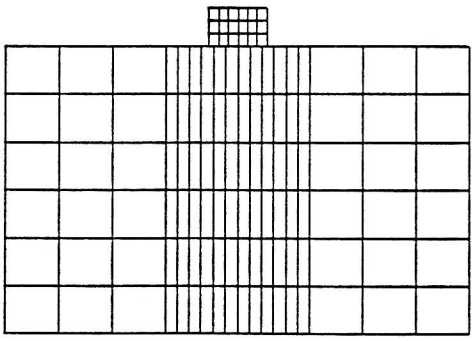

MC4

Fig. 5.2.2 Rigid punch on elastic foundation; discretizations

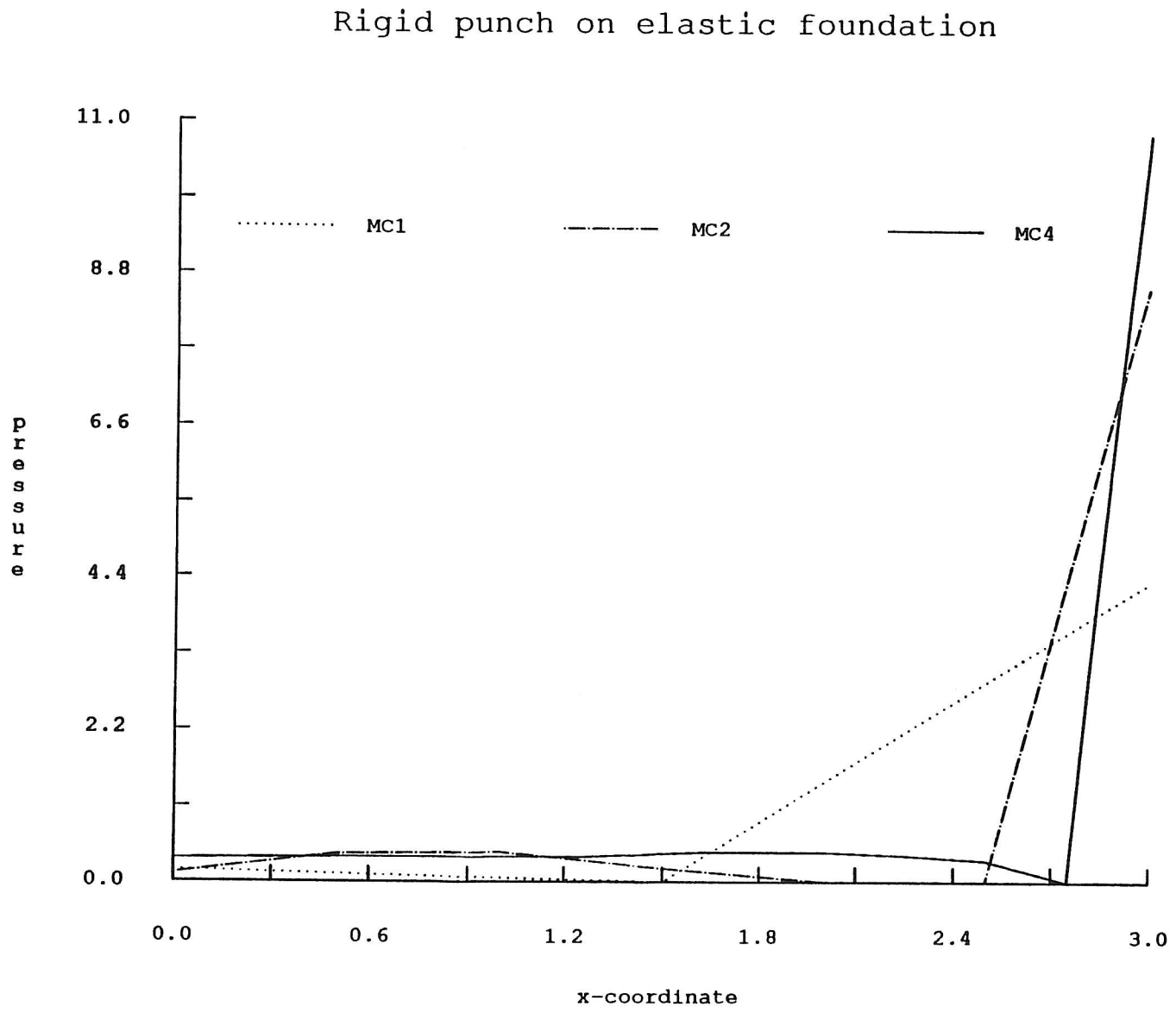

Fig. 5.2.3 Rigid punch on elastic foundation; pressure distribution

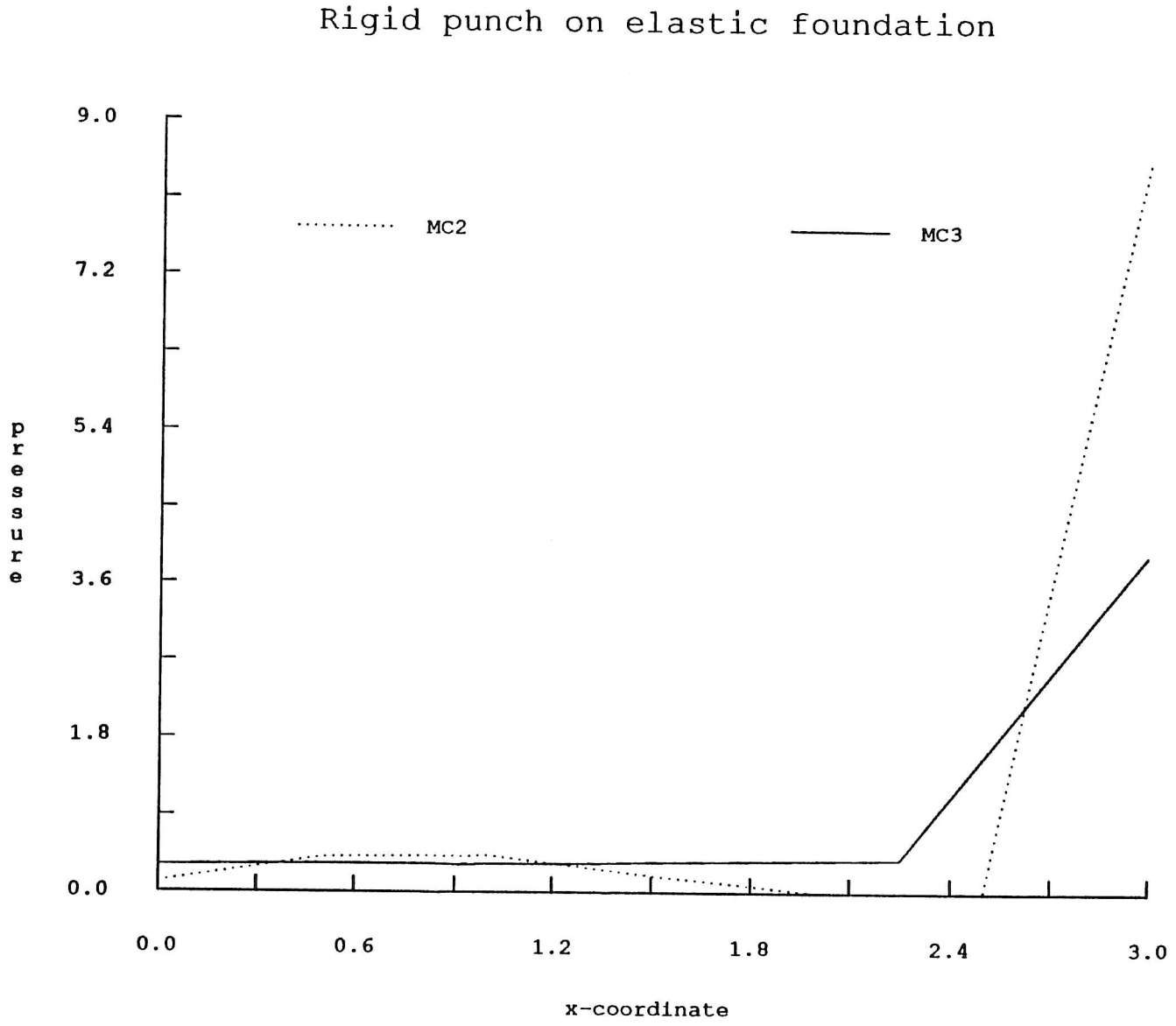

Fig. 5.2.4 Rigid punch on elastic foundation; pressure comparison

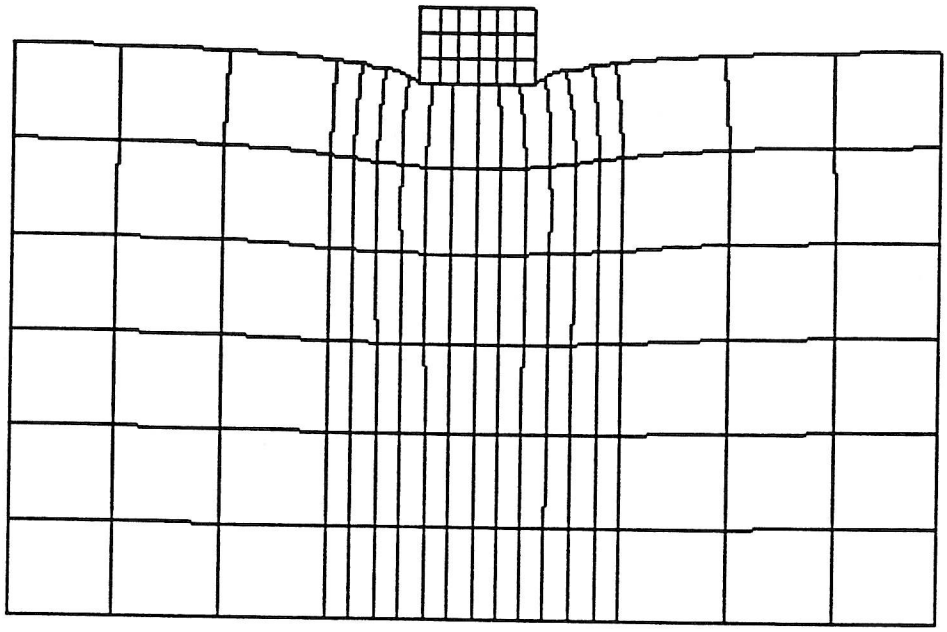

scale 1:40

Fig. 5.2.5 Rigid punch on elastic foundation;
deformed shape (mesh MC4)

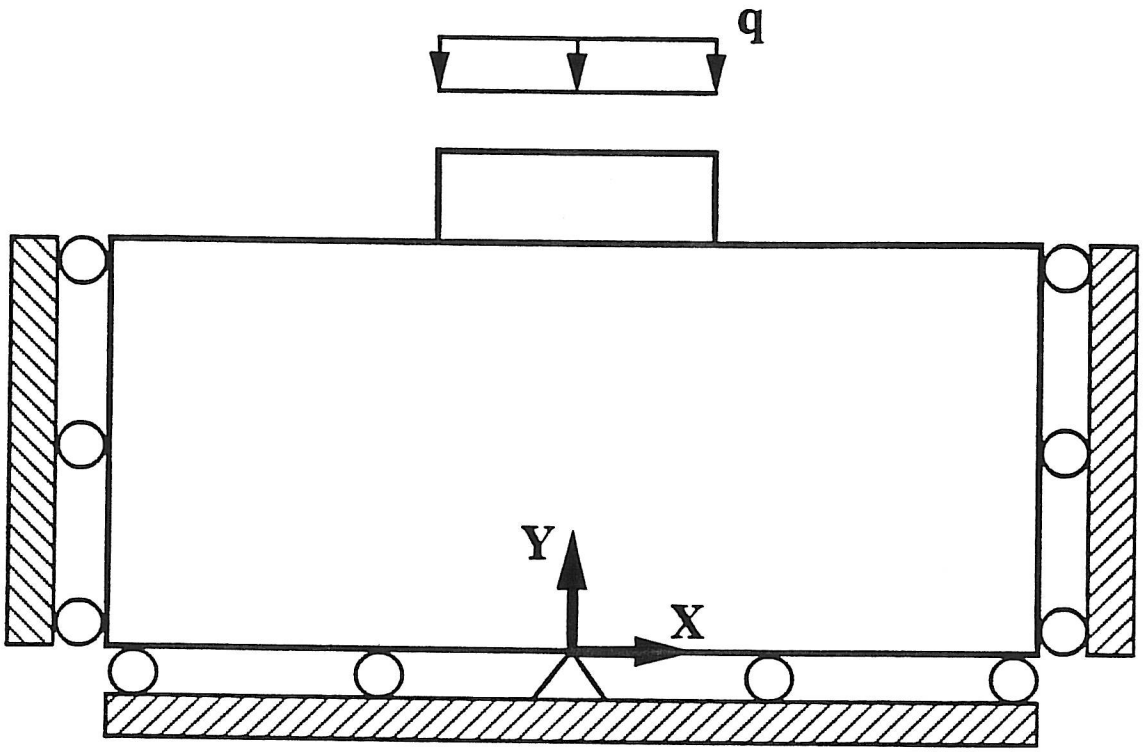

Fig. 5.3.1 Elastic punch on elasto-plastic foundation

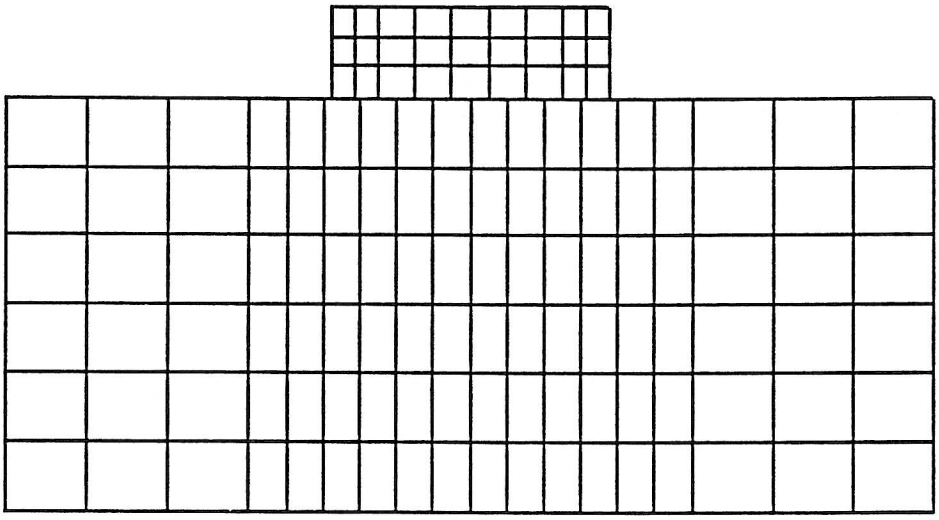

Fig. 5.3.2 Elastic punch on elasto-plastic foundation; discretization

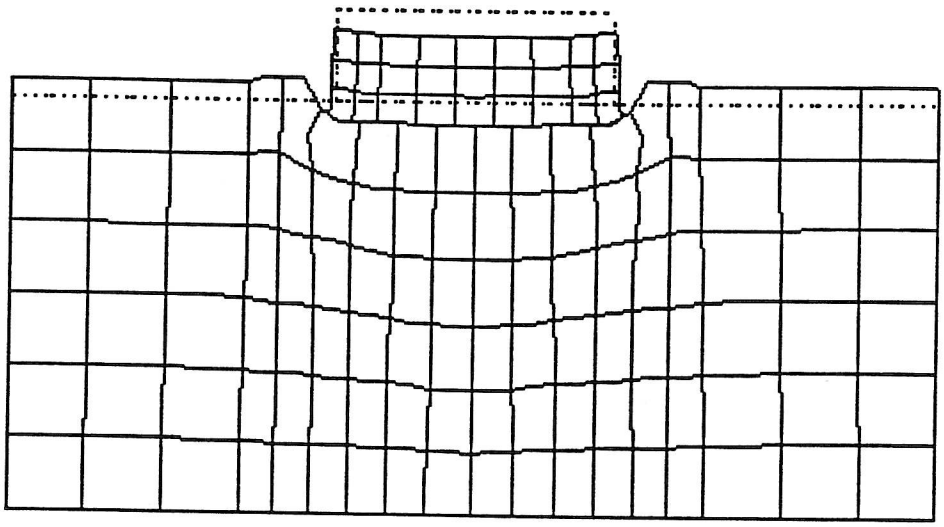

scale 1:10

Fig. 5.3.3 Elastic punch on elasto-plastic foundation;
deformed shape (q=25)

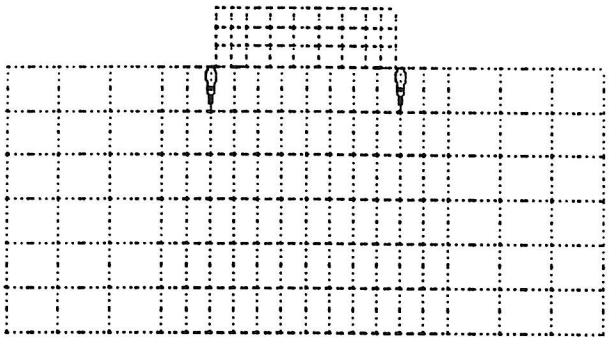

q= 10

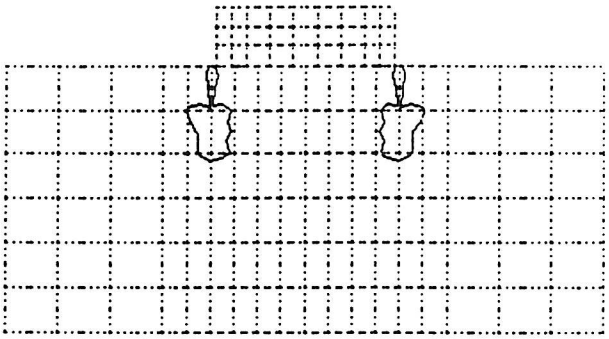

q= 15

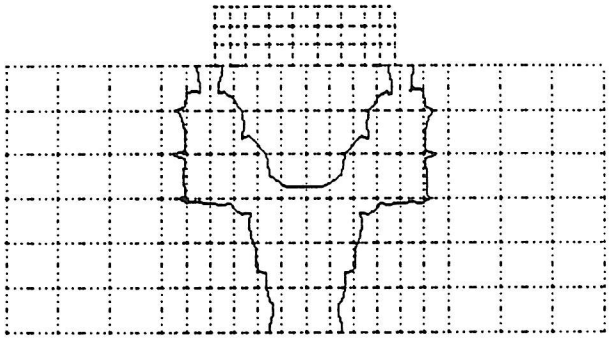

q= 20

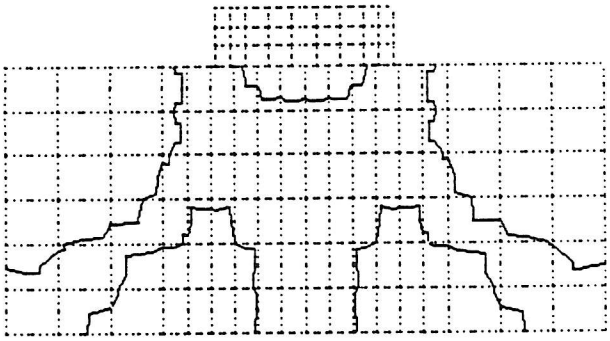

q= 25

Fig. 5.3.4 Elastic punch on elasto-plastic foundation; evolution of plastic deformation

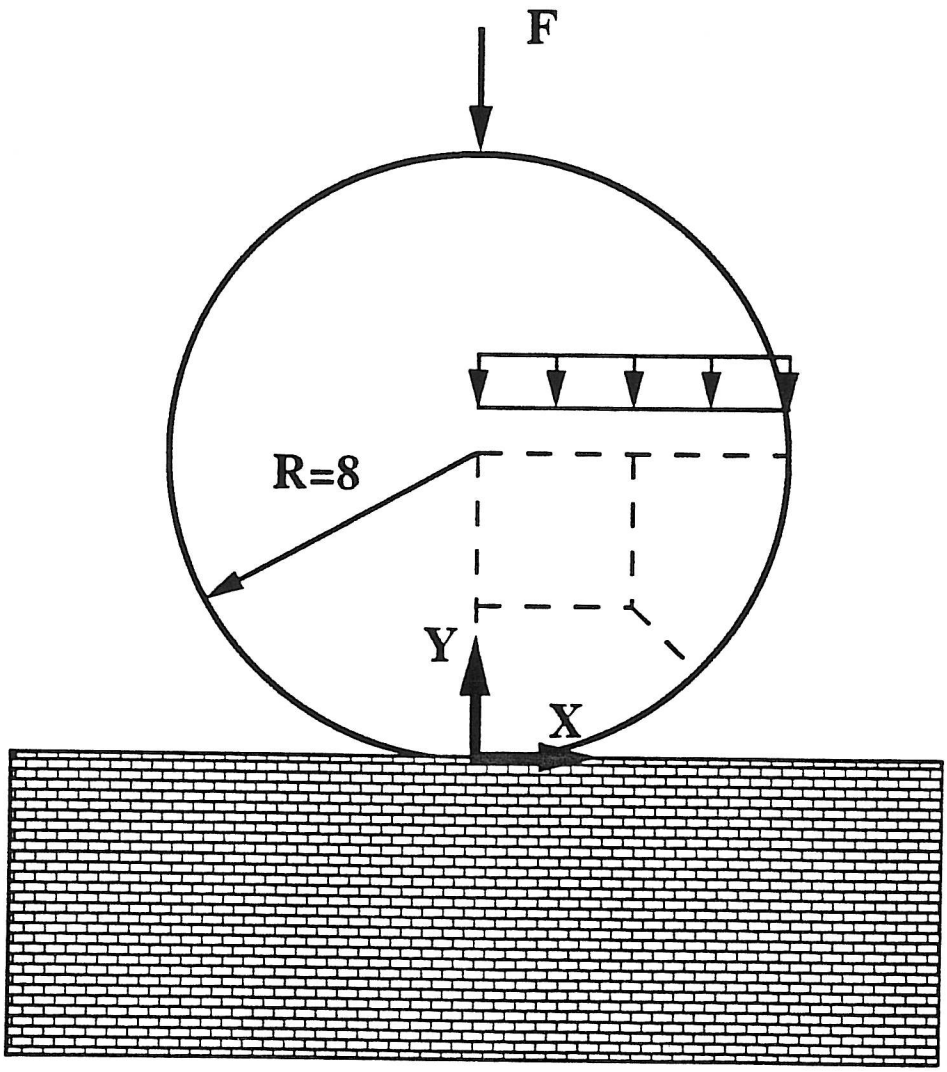

Fig. 5.4.1 Cylinder on rigid foundation

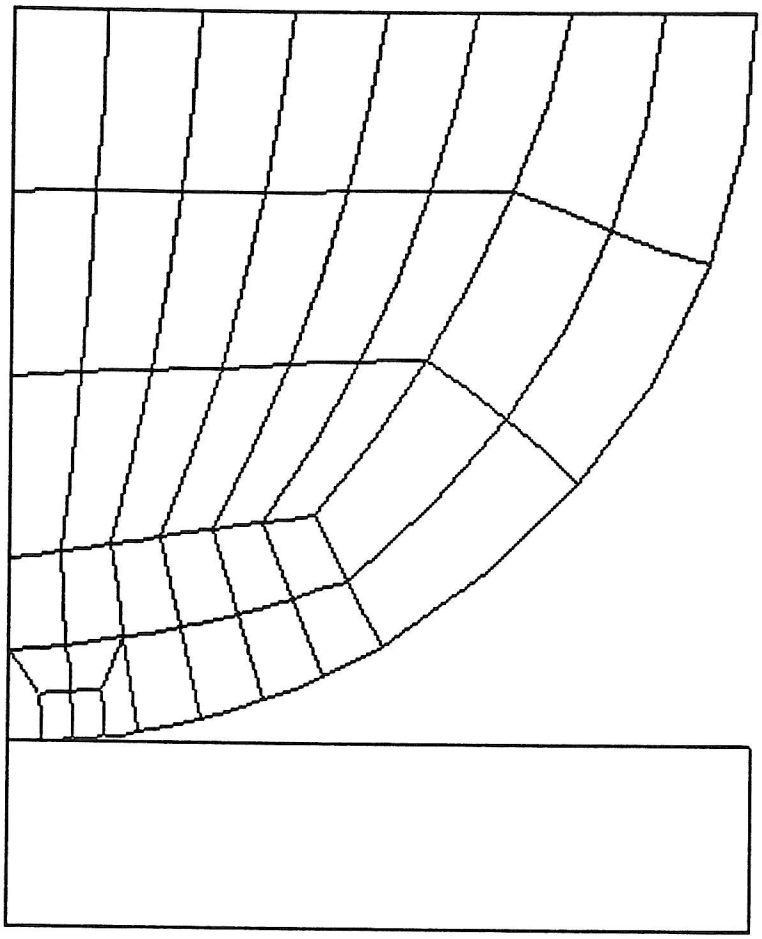

Fig. 5.4.2 Cylinder on rigid foundation; discretization

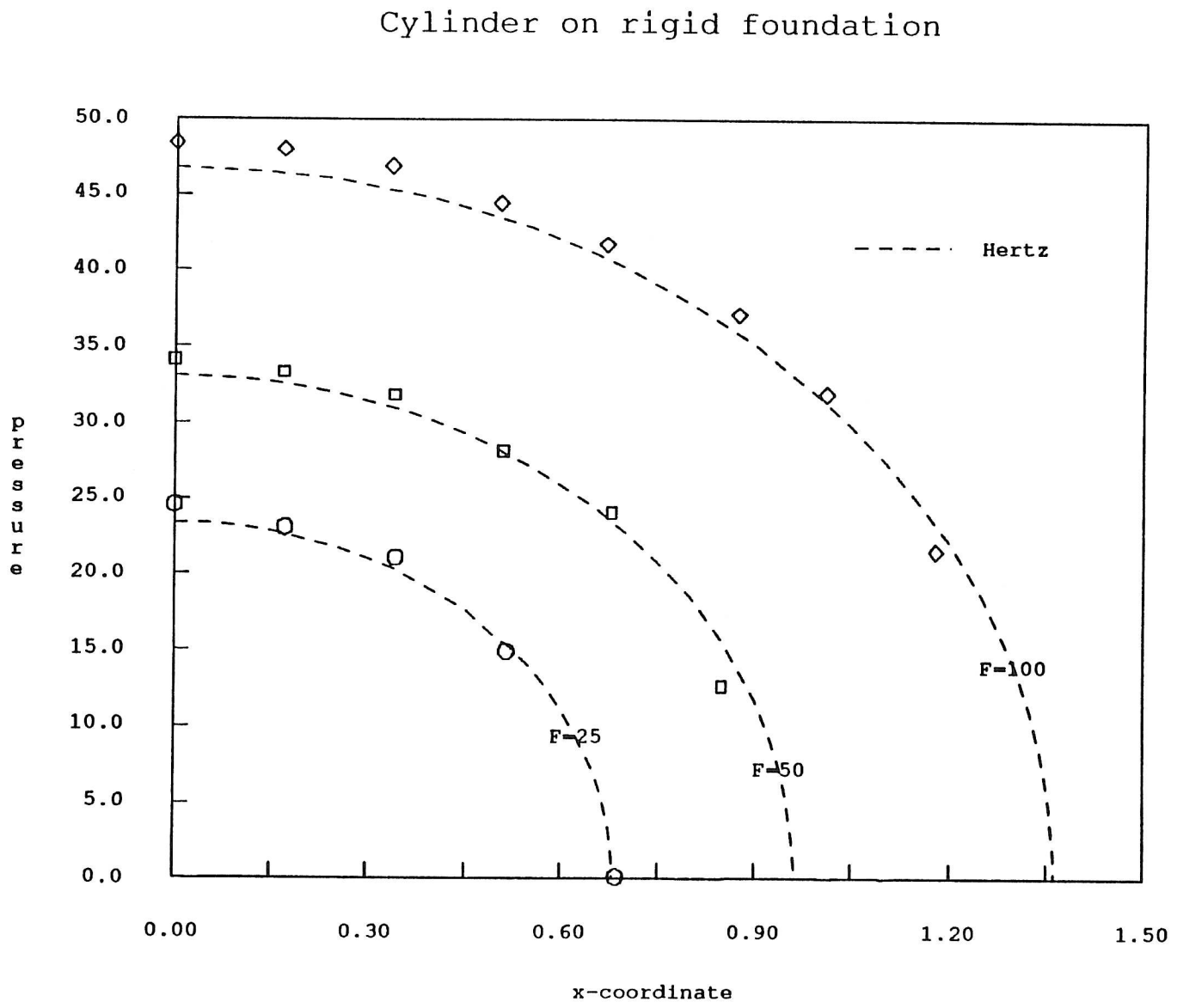

Fig. 5.4.3 Cylinder on rigid foundation; pressure distribution

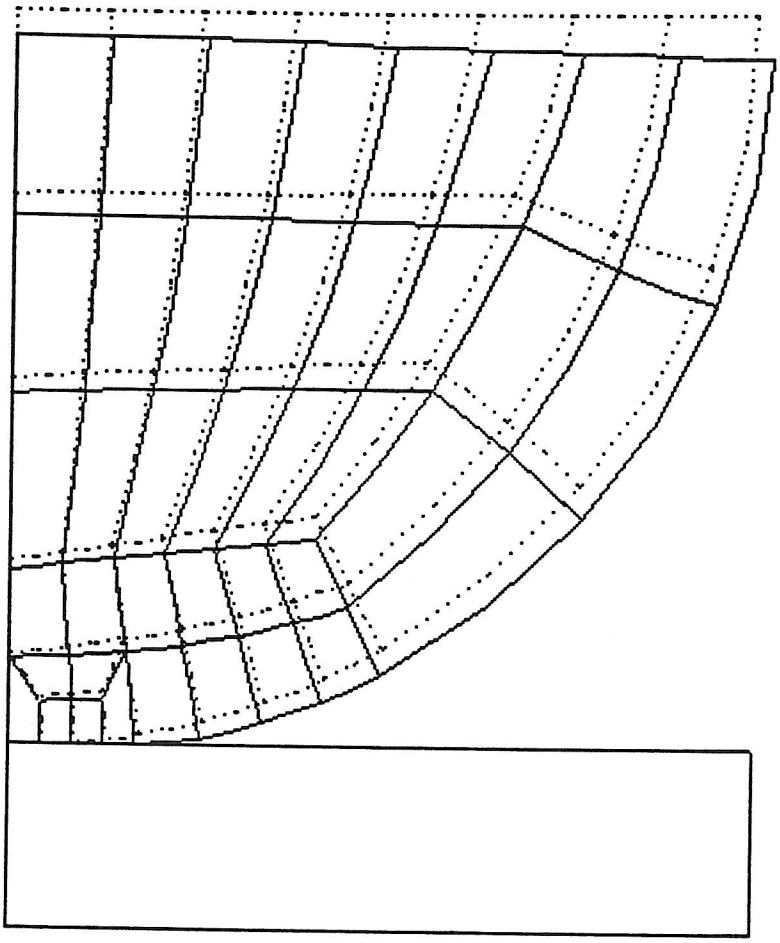

scale 1:1

Fig. 5.4.4 Cylinder on rigid foundation; deformed shape (F=100)

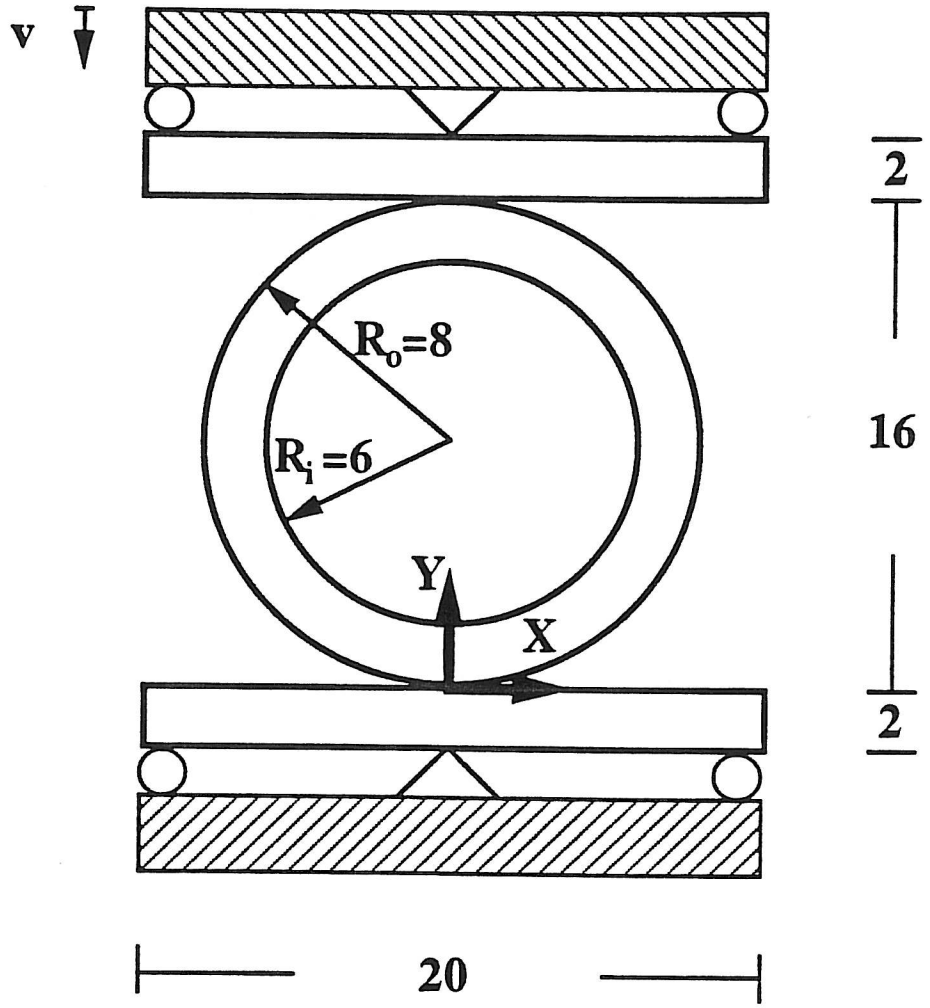

Fig. 5.5.1 Ring on elastic foundation

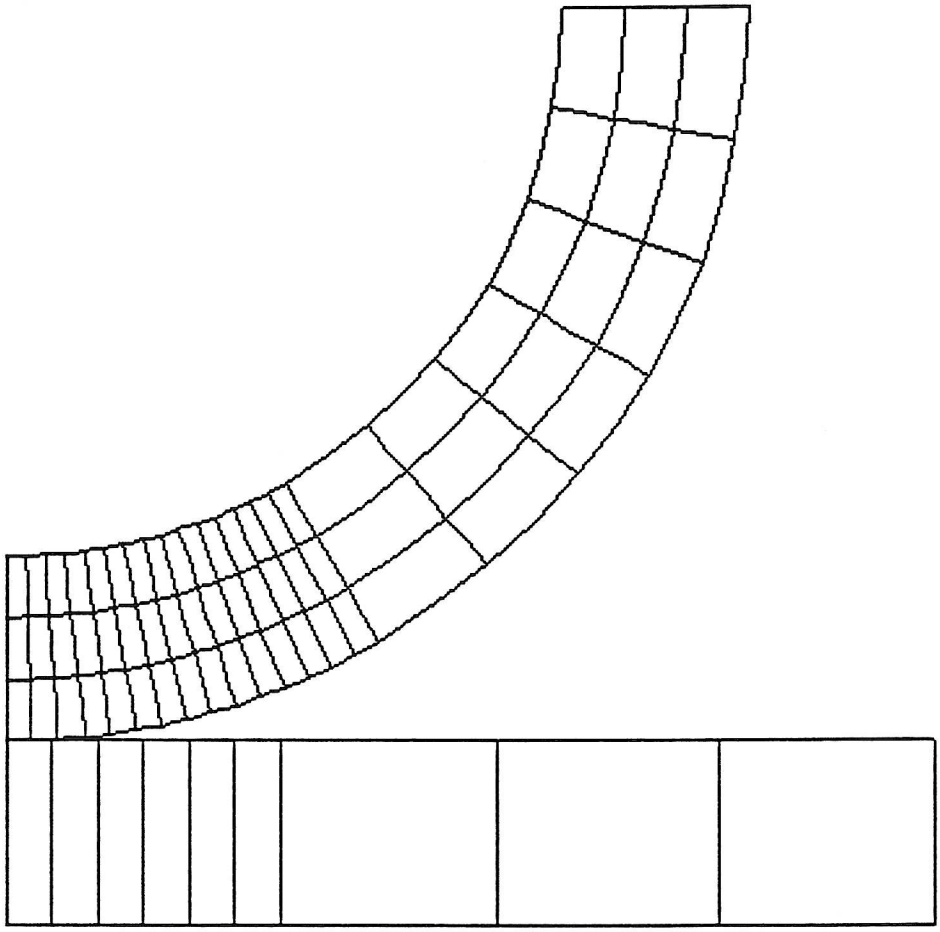

Fig. 5.5.2 Ring on elastic foundation; discretization

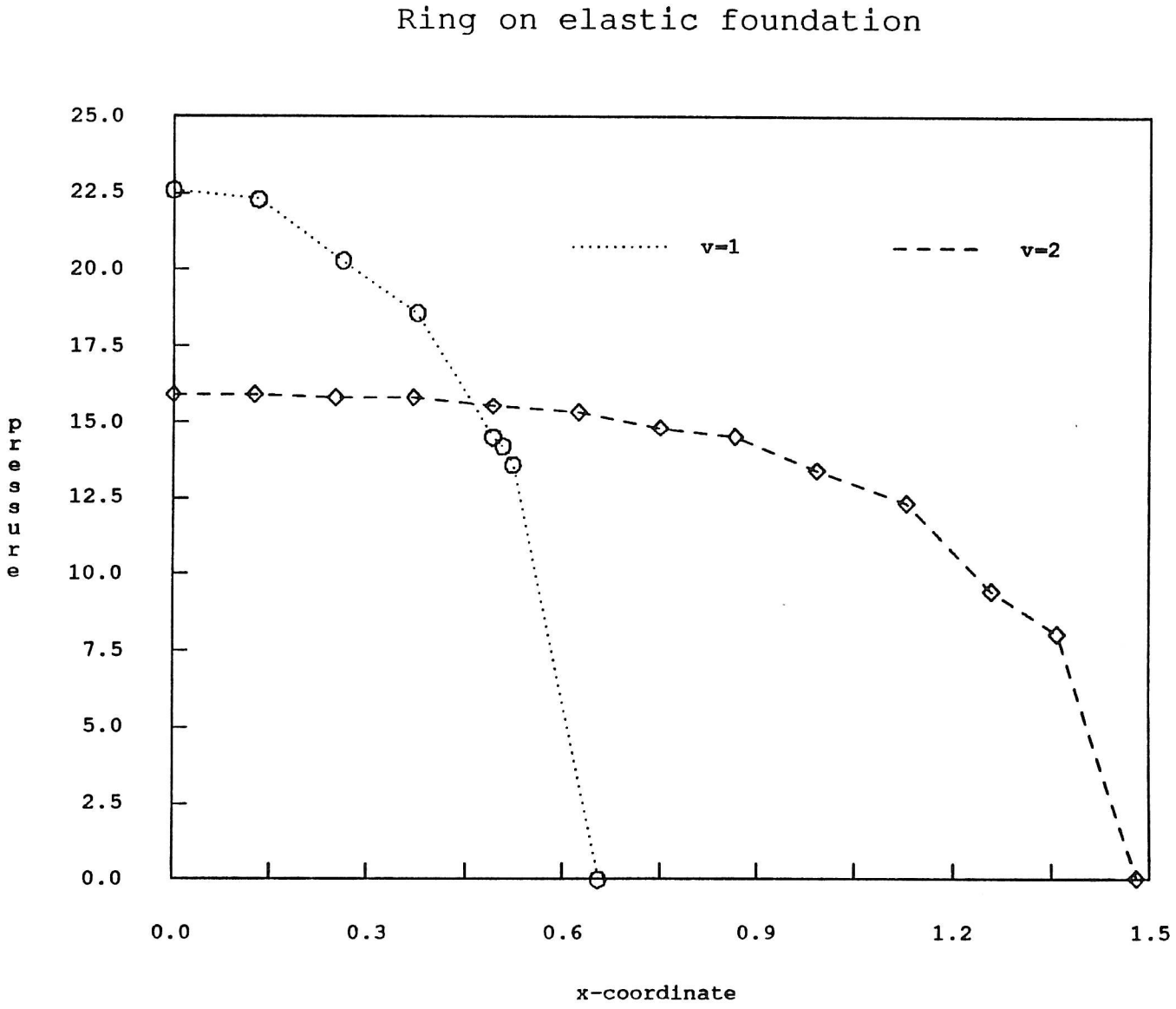

Fig. 5.5.3 Ring on elastic foundation; pressure distribution

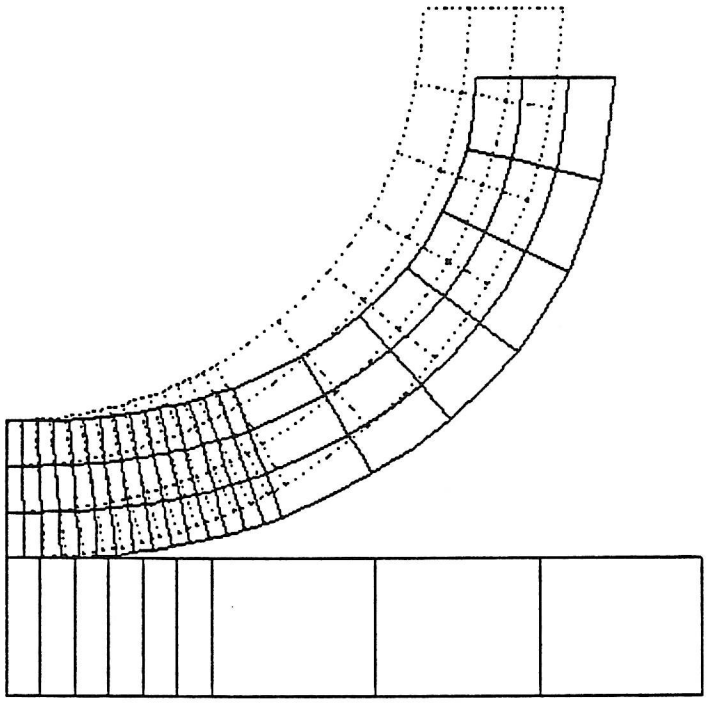

v= 1

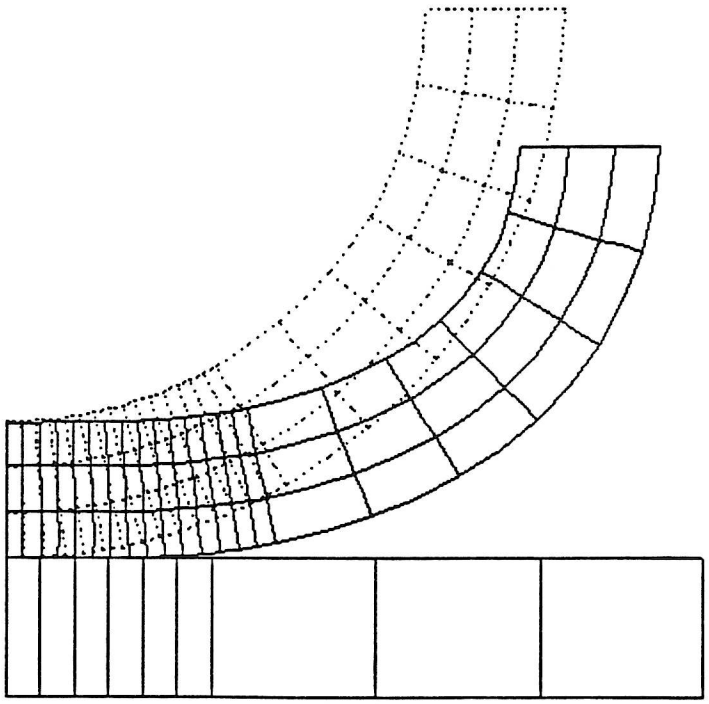

v= 2

scale 1:1

Fig. 5.5.4 Ring on elastic foundation; deformed shapes